Order-by-Disorder and Quantum Coulomb Phase in Quantum Square Ice

Louis-Paul Henry[1] and Tommaso Roscilde[1,2]

[1]*Laboratoire de Physique, CNRS UMR 5672, Ecole Normale Supérieure de Lyon,
Université de Lyon, 46 Allée d'Italie, Lyon, F-69364, France*
[2]*Institut Universitaire de France, 103, boulevard Saint-Michel 75005 Paris, France*

We show that quantum square ice—namely, the two-dimensional version of proton or spin ice with tunable quantum tunneling of the electric or magnetic dipole moment—exhibits a quantum spin-liquid phase supporting fractionalized spinons. This phase corresponds to a thermally induced, deconfined quantum Coulomb phase of a two-dimensional lattice gauge theory. It emerges at finite, yet exceedingly low temperatures from the melting of *two* distinct order-by-disorder phases appearing in the ground state: a plaquette valence-bond solid for low tunneling; and a canted Néel state for stronger tunneling. The latter phases appear via the highly nonlinear effect of quantum fluctuations within the degenerate manifold of ice-rule states, and they can be identified as the two competing ground states of a discrete lattice gauge theory (quantum link model) emerging as the effective Hamiltonian of the system within degenerate perturbation theory.

Introduction.—Frustrated magnetism represents a unique test bed for the investigation of quantum effects at the macroscopic scale [1,2]. Indeed classical models of frustrated magnetism can exhibit macroscopically degenerate ground states (so-called classical spin liquids [2]), seemingly violating the third principle of thermodynamics. As a consequence, only quantum fluctuations can decide what ground state and macroscopic low-energy physics will ultimately emerge in the system. The exponential degeneracy of the ground state is a feature of fundamental models of magnetism in condensed matter, such as spin ice—the magnetic analog of proton ice [3]—whose ground states satisfy a local constraint (the so-called ice rule), and it is also a feature of lattice gauge theories (LGTs) [4,5] inspired by high-energy physics. The ground-state ambiguity left over by classical physics can be resolved by quantum fluctuations via a most appealing scenario, namely, the appearance of a quantum spin-liquid state without long-range order, and featuring fractionalized excitations [2]. This mechanism is in fact proven rigorously for lattice gauge theories [4–6], in which spin-liquid states correspond to a deconfined phase of the theory, and unbound charges correspond to fractionalized excitations. In quantum magnetism the situation is more complex, as quantum fluctuations can often promote long-range order in the ground state (as well as conventional excitations) via an order-by-disorder mechanism [7,8]; yet mounting numerical and experimental evidence is appearing in favor of spin-liquid phases in fundamental models of magnetism [9], including quantum spin ice [10–14], in relationship with deconfined phases of an emerging LGT.

In the present Letter, we show that square ice—the two-dimensional version of pyrochlore ice, realized in very different experimental settings [15]—exhibits an intriguing competition between order-by-disorder and spin-liquid physics, when quantum tunneling of the electric or magnetic dipole moments of ice is introduced in the system. On the one hand, the ground state exhibits *two* competing order-by-disorder phases, that can be identified with the confined phases of an emergent U(1) LGT. Yet an arbitrarily low temperature can drive a transition towards a so-called quantum Coulomb phase [10,13] supporting deconfined spinons as elementary excitations, and corresponding to a finite-temperature realization of a U(1) spin liquid in two dimensions.

Quantum square ice.—Square spin ice with quantum tunneling of the magnetic moments can be modeled as the antiferromagnetic transverse-field Ising model (TFIM) on a checkerboard lattice [Fig. 1(a)]:

$$\mathcal{H} = J\sum_{\boxtimes}(\sigma_{\boxtimes}^z)^2 - \Gamma\sum_i \sigma_i^x, \qquad (1)$$

where the first sum runs over the crossed plaquettes (vertices) of the checkerboard lattice [see Fig. 1(a)], and $\sigma_{\boxtimes}^z = \sum_{i\in\boxtimes}\sigma_i^z$; $\sigma_i^{x(z)}$ are Pauli matrices. In classical square ice ($\Gamma = 0$), the ensemble of degenerate ice-rule ground states—with vanishing magnetization on each crossed plaquette—realizes a $2d$ Coulomb phase [16]. Such a phase is characterized by algebraic spin-spin correlations (decaying as r^{-2}) [17] with a peculiar signature in the spin structure factor in the form of *pinch points* [18], and by deconfined monopolelike excitations. When introducing quantum tunneling via a transverse field Γ, a perturbative treatment of the quantum term to the lowest order leads to a model of *frustrated* compact lattice QED (fcQED) for a discrete ($S = 1/2$) gauge field [10,19]—also known as the U(1) quantum link model or U(1) gauge magnet [20] in the high-energy physics literature:

$$\mathcal{H}_{\text{eff}}^{(4)} = -K_4 \sum_\square F_\square + \text{const.} \qquad (2)$$

Here the sum runs over the (uncrossed) plaquettes, and $F_\square = \sigma_1^+ \sigma_2^- \sigma_3^+ \sigma_4^- + \text{H.c.}$ is the plaquette flip operator (the indices run counterclockwise around the plaquette). The coupling constant has the value $K_4 = 20[\Gamma^4/(2J)^3]$, where the factor of 20 accounts for all the possible sequences of elementary spin flips leading to a plaquette flip, and creating either one or two monopole pairs as virtual intermediate excitations [21]. fcQED can be suspected to undergo confinement due to the Polyakov mechanism valid for ordinary (nonfrustrated) compact QED in $d = 2$ [19,32]. This expectation is indeed verified by numerics [33–35], finding that the Coulomb phase is removed from the ground state of fcQED in favor of a gapped plaquette valence-bond solid [pVBS—see Fig. 1(b)]. As we will see, considering a field of arbitrary strength leads to a richer physics, related to the emergence of a more complex emerging LGT.

Method.—A Trotter-Suzuki decomposition [36] with M Trotter steps at an inverse temperature β maps the quantum partition function of quantum square ice, Eq. (1), onto the partition function of stacked spin-ice planes with reduced couplings J/M, and interacting via ferromagnetic couplings of strength $J_\tau = -\log[\tanh(\beta\Gamma/M)]/(2\beta)$. This mapping has the advantage that the efficient loop algorithm for spin ice [37] can be generalized to the quantum context, where it takes the form of a *membrane* algorithm: a loop of spin flips (or an open string in the presence of monopole excitations) is first created at a given imaginary time, and then propagated along the imaginary-time direction as in a $1d$ Wolff algorithm [21]. The resulting dynamics allows us to explore efficiently the delicate coexistence between kinematic constraints and quantum fluctuations; the introduction of the membrane move turns out to be crucial for the correct equilibration of the system, similar to what is observed for the loop move in the classical case. Our quantum Monte Carlo (QMC) simulations are performed on $L \times L$ lattices with sizes ranging up to $L = 32$.

Phase diagram.—Figure 2 shows the phase diagram of the system in the field-temperature plane. Notice the logarithmic temperature scale, emphasizing that salient features occur at very low temperatures. Upon increasing the field, the system's ground state is driven from a Coulomb phase for $\Gamma = 0$ to a pVBS phase, for $\Gamma/J \lesssim 0.25$, to a canted Néel phase for $0.25 \lesssim \Gamma/J \lesssim 0.55$, and finally to a quantum paramagnetic phase for $\Gamma/J \gtrsim 0.55$. The pVBS phase and Néel phase melt at a finite critical temperature, which has been determined as described below.

VBS transition and fcQED.—As already mentioned, the appearance of a pVBS phase has been proven numerically [33,34] for fcQED, emerging as the effective Hamiltonian of quantum square ice at the lowest (4th) order in the field. The characteristic ordered structure of the pVBS state corresponds to the appearance of a staggered pattern of local resonances between a plaquette Néel state $|N\rangle = |\uparrow_1 \downarrow_2 \uparrow_3 \downarrow_4\rangle$ and its spin-flipped partner $|\bar{N}\rangle$ [Fig. 1(b)]. Such an ordered structure can be captured by the *flippability*, namely, the average value of the projector onto flippable (= Néel) plaquette states $f_\square = \langle |N\rangle\langle N| + |\bar{N}\rangle\langle \bar{N}| \rangle = \langle F_\square^2 \rangle$. Detecting directly the onset of pVBS order for the TFIM Hamiltonian of Eq. (1) turns out to be prohibitive from the numerical point of view, given that pVBS order occurs at a temperature $T/J \sim (\Gamma/J)^4$ lying several orders of magnitude below the energy scale of the spin-spin coupling. We rather focus on the effective Hamiltonian Eq. (2), and calculate its thermal phase transition to pVBS order via QMC calculations [21]—for such a system, the membrane

FIG. 1 (color online). (a) Checkerboard lattice, showing the notation for the lattice-site indices and for the vertex indices, as well as a classical ice-rule configuration plus a monopole pair; (b), (c) Sketch of the ordered ground-state phases of quantum square ice. The squares in the pVBS phase indicate resonating states of the kind $(|N\rangle + |\bar{N}\rangle)/\sqrt{2}$ (see main text for the notation).
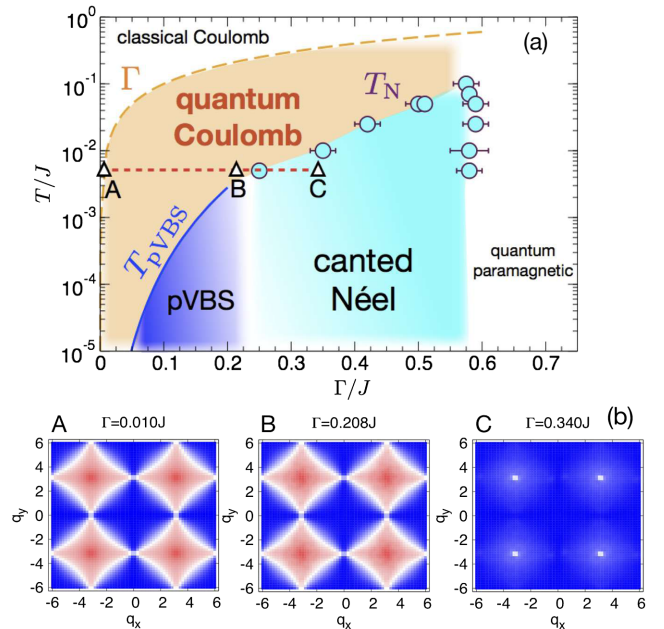
FIG. 2 (color online). (a) Phase diagram of quantum square ice; boundaries of the pVBS phase (T_{pVBS}) and of the canted Néel phase (T_N) have been obtained as described in the main text; the dashed line marks a crossover from coherent to diffusive spinon or monopole dynamics at the energy scale set by the transverse field Γ. (b) Static structure factor for a system with $L = 24$, corresponding to the (Γ, T) parameters as indicated in panel (a).

algorithm is the only possible update compatible with the kinematic constraints. Using the crossing of the Binder cumulants for the staggered flippability [21] we determine the critical temperature for the melting of the pVBS state as $T_{\text{pVBS}}/J = 1.80(3)(\Gamma/J)^4$. This estimate allows us to draw the curve shown in Fig. 2.

Néel transition.—In the case of the Néel phase, we have considered systematic finite-size extrapolations of the staggered magnetization, estimated as $m_s = (1/L^2)\langle|\sum_i(-1)^i\sigma_i^z|\rangle$, where L is the linear size of the system. Figure 3 shows polynomial fits to the finite-size dependence of the magnetization, exhibiting a very small ($\sim 10^{-2}$) albeit finite staggered moment in the thermodynamic limit. The vanishing of m_s leads to the estimate of the line of Néel critical temperatures T_N. The upper critical field estimated via the vanishing of the order parameter is found to be consistent with the position of an inflection point in the transverse magnetization (see Fig. 5).

Néel phase from the effective Hamiltonian.—The appearance of the Néel phase is a highly nontrivial order-by-disorder phenomenon, as it is associated with diagonal order induced by a purely nondiagonal operator (the transverse field term)—and, paradoxically, it appears only if the transverse field is sufficiently strong, while at weak fields the order is rather off diagonal. One might suspect that such a phase is already present in the classical ($S \to \infty$) limit of the TFIM due to an order-by-disorder mechanism induced by thermal fluctuations; we have explicitly checked this aspect [21] and we do not find any form of magnetic order in the classical, continuous spin version of Eq. (1) at small but finite temperature. Moreover the Néel phase is not stabilized by harmonic quantum fluctuations, as verified explicitly within spin-wave theory in Ref. [38]. We can only gain understanding of this phase when going beyond the lowest-order perturbative Hamiltonian of Eq. (1), and considering further perturbation terms. One can do so systematically following, e.g., Ref. [39]—see Ref. [21] for an extensive discussion. To gain a quantitative understanding of the Néel phase, it turns out that it is necessary to push the perturbative expansion up to the 8th order in the magnetic field; to this order the effective Hamiltonian—obtained by considering

FIG. 3 (color online).   (a) Scaling of the Néel order parameter at $T/J = 10^{-2}$; solid lines are fits to cubic polynomials; (b) Scans in the static structure factor at $T/J = 5 \times 10^{-3}$ and $L = 24$, showing the evolution of the pinch-point width.

exclusively virtual processes involving the creation or annihilation of a single monopole pair—reads

$$\mathcal{H}_{\text{eff}}^{(8)} = -K_4\sum_\square F_\square - K_6\sum_{l\in\mathcal{L}_6}F_{6l}$$
$$- K_8\sum_{l\in\mathcal{L}_8}F_{8l} - K_8'\sum_\square F_\square^2 + \text{const.} \quad (3)$$

Here $F_{nl} = \sigma_1^+\sigma_2^-\ldots\sigma_{n-1}^+\sigma_n^- + \text{H.c.}$ is the operator flipping the spins (in alternate fashion) on a loop l, belonging to the family $\mathcal{L}_n$ of loops of length n. The coefficients $K_n = a_n\Gamma^n/(2J)^{n-1}$ are given explicitly in Ref. [21]. The last term is a purely *diagonal* term, which amounts to counting the number of flippable plaquettes, and therefore its energy is minimized by the Néel state, being the maximally flippable state [7,40]. Hence, we can expect that the pVBS-Néel transition is fundamentally driven by the competition between the 4th order term and the diagonal 8th order term [21].

Quantum Coulomb phase.—Finally, we focus on the thermally disordered phase in quantum square ice. As already mentioned in the introduction, pinch points with *zero* width in the static structure factor $S(\boldsymbol{q}) = (1/N)\sum_{ij}e^{i\boldsymbol{q}\cdot(\boldsymbol{r}_i-\boldsymbol{r}_j)}\langle\sigma_i^z\sigma_j^z\rangle$ are a consequence of algebraic spin-spin correlations of the classical Coulomb phase of $2d$ spin ice [18], which are in turn a characteristic feature of the spatial correlations of the divergenceless magnetization field of square ice [21]. Figure 2(b), A and B and Fig. 3 show that, for a weak field and low temperatures, pinch-point features (with a resolution limited width up to system sizes $L = 24$, Fig. 3) survive in the structure factor. This shows that a finite temperature minimally affects correlations in this regime, as well as the finite concentration of monopoles induced by the transverse field. Indeed field-induced monopole pairs are strongly off resonant (as $\Gamma \ll 2J$), and hence they form bound states, screening each other and leaving correlations unaffected.

The Coulomb-phase correlations exhibited at low T and finite Γ are a clear indication of the deconfined nature of its excitations. Indeed, despite the confined nature of the ground-state phases of quantum square ice, the temperature leads to a confinement-deconfinement transition [19] when it exceeds the critical temperatures T_{pVBS} and T_N for the melting of the low-T ordered phases. We can directly probe the fractionalization of single spin flips into monopoles by performing simulations in a modified ensemble, determining the statistical properties of a pair of monopoles injected in the system via a spin flip, and subject to the quantum and thermal fluctuations of the underlying spin network (which represents the *gauge field*—see below). If the QMC dynamics is constrained to preserve the two monopoles [41], one can reconstruct the probability $p(r)$ that the monopoles are at given distance r [normalized so that $\int dr(2\pi r)p(r) = 1$]. Figure 4 shows that the probability $p(r)$ at a temperature $T/J = 10^{-2}J$ is minimally affected by the presence of quantum fluctuations—both for $\Gamma = 0$ and $\Gamma \approx 0.2J$ we
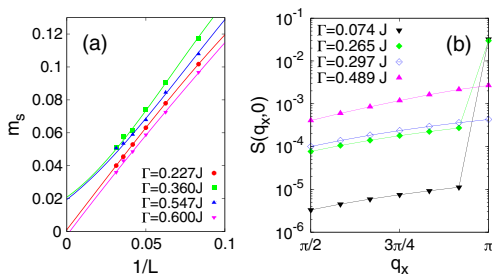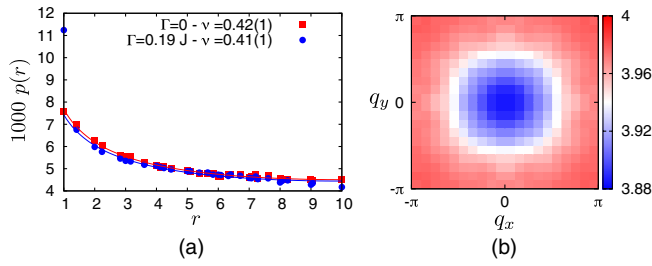
FIG. 4 (color online).   (a) Distribution of monopole separation $p(r)$ at $T = 10^{-2}J$ in the classical ($\Gamma = 0$) and quantum Coulomb phase ($\Gamma = 0.188J$) for a system size $L = 20$. Solid lines are fits to $A[r^{-\nu} + (L-r)^{-\nu}]$; (b) Bottom of the two-spinon continuum (Δ_q) in the quantum Coulomb phase ($\Gamma = 0.188J, T = 10^{-2}J, L = 20$).

find that $p(r) \sim r^{-a}$ with $a \approx 0.4$, which implies deconfined pairs with $\langle r \rangle = \infty$ in the thermodynamic limit.

Despite sharing the same deconfinement properties, a fundamental difference exists between the monopole excitations at finite Γ with respect to those of the classical limit $\Gamma = 0$. Indeed Γ represents a hopping term for the monopoles, which are therefore turned into coherent *spinons* with a finite bandwidth. The finite bandwidth for spinons can be detected numerically by looking at the dispersion of the minimum gap Δ_q for spin flips, obtained via the asymptotic decay of the imaginary-time correlation function $\langle S_q^x(0) S_{-q}^x(\tau) \rangle \sim \exp(-\Delta_q \tau)$ [21]. Δ_q provides the lower bound to the two-spinon continuum in the dynamic structure factor, and it clearly shows a dispersion with bandwidth $\sim \Gamma$ around the classical spin-flp energy of $4J$. Because of the evidence of thermally deconfined spinons, we call this regime a thermally induced *quantum Coulomb phase*, whose short-range properties are identical to those of a U(1) spin-liquid phase (the latter being realized strictly speaking only in $3d$ at $T = 0$ [10]). In particular we expect an algebraic spin-liquid behavior to persist up to a length $l_{\rm th} \sim \exp(2J/T)$ given by the average distance between *thermally* excited spinon pairs; it is easy to verify that this length can be astronomically large. The quantum Coulomb phase transforms smoothly into the classical Coulomb phase for temperatures $T \sim J$, at which the de Broglie wavelength of the spinons becomes smaller than the lattice step, and their dynamics becomes diffusive—as also revealed by QMC calculations [21].

Gauge mean-field theory.—The picture of a quantum Coulomb phase is further corroborated by a theoretical treatment of quantum square ice based on the recently introduced gauge mean-field theory (gMFT) [13]. The latter approach formally splits the $S = 1/2$ spin degrees of freedom into a "matter" part—the spinon field, represented by a bosonic field of integer modulus $\Phi_r = e^{i\phi_r}$—existing on the centers r of the vertices, and a gauge part—the $S = 1/2$ spin gauge field $s_{rr'}^\alpha$, with $\alpha = x, y, z$—living on the sites of the lattice which are in between two vertices r, r' [see Fig. 1(a)]. A mean-field decoupling of the gauge field with respect to the spinon field leads to the

following Hamiltonian, $\mathcal{H} \approx \mathcal{H}_\Phi + \mathcal{H}_s + \text{const}$, [21] with $\mathcal{H}_\Phi = -2\Gamma \sum_{\langle rr' \rangle} \langle s_{rr'}^x \rangle \cos(\phi_r - \phi_{r'}) + 4J \sum_r Q_r^2$ and $\mathcal{H}_s = -2\Gamma \sum_{\langle rr' \rangle} \langle \cos(\phi_r - \phi_{r'}) \rangle s_{rr'}^x$. Here Q_r is the conjugate (charge) operator to the spinon phase, $[\phi_r, Q_r] = i$. In particular $\mathcal{H}_s$ is readily minimized by a state with $\langle s^x \rangle = 1/2$, reducing the spinon Hamiltonian $\mathcal{H}_\Phi$ to a *quantum rotor Hamiltonian* on the square lattice. Within this mapping the transverse magnetization is simply related to the kinetic energy of the bosonic spinons, namely, $\langle \sigma^x \rangle = \langle \cos(\phi_r - \phi_{r'}) \rangle$. Remarkably, the quantum rotor Hamiltonian admits a numerical solution via QMC [21], which allows us to compare quantitatively the predictions of gMFT with the exact results coming from the QMC simulation of quantum square ice. This comparison is made in Fig. 5, clearly showing that $T = 0$ gMFT is quantitatively accurate in the quantum Coulomb phase, while it deviates from the numerically exact results for quantum square ice precisely when the system enters the Néel phase. In particular, gMFT represents the low-field phase for the matter sector of quantum square ice as a bosonic *Mott insulator*, with a gap corresponding to the spinon gap, and spinon pairs representing particle-hole pairs of the Mott insulator. The elementary excitations of a bosonic Mott insulator are gapped, deconfined particle-hole pairs forming a continuum [42]. Therefore, this result further corroborates the picture in which the excitation spectrum for the matter sector of the quantum Coulomb phase consists of a continuum of deconfined spinons.

Experimental realization.—The most prominent experimental platform for the realization of quantum square ice is represented by microtrapped ions, which naturally implement transverse-field Ising models in different planar geometries [43]; an alternative scheme might rely on tailored nanomagnets [44]. The long-range interactions in these systems are expected to have a marginal impact on the quantum Coulomb phase as long as the low-T symmetry breaking phase melts at a critical temperature $T_c \ll \Gamma$. This suggests that atomic physics or solid-state quantum simulators offer promising platforms for the implementation of fundamental phenomena of lattice gauge theories, as recently proposed in the context of neutral
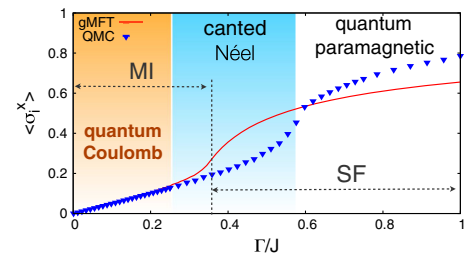
FIG. 5 (color online).   Transverse magnetization of quantum square ice for $T/J = 5 \times 10^{-3}$ and $L = 16$, compared with the gauge mean-field theory (gMFT) prediction. The vertical dashed line marks the transition from Mott insulator (MI) to superfluid (SF) in the corresponding quantum rotor model (see text).

atoms [45–47], with special emphasis on U(1) quantum link models [35,45,47].

[1] *Introduction to Frustrated Magnetism: Materials, Experiments, Theory*, edited by C. Lacroix, F. Mila, and P. Mendels (Springer, Berlin, 2011).

[2] L. Balents, Nature (London) **464**, 199 (2010).

[3] C. Castelnovo, R. Moessner, and S. Sondhi, Annu. Rev. Condens. Matter Phys. **3**, 35 (2012).

[4] J. Kogut, Rev. Mod. Phys. **51**, 659 (1979).

[5] J. Kogut, Rev. Mod. Phys. **55**, 775 (1983).

[6] A. Y. Kitaev, Ann. Phys. (Amsterdam) **303**, 2 (2003).

[7] R. Moessner and S. L. Sondhi, Phys. Rev. B **63**, 224401 (2001).

[8] E. F. Shender and S. A. Kivelson, Phys. Rev. Lett. **66**, 2384 (1991).

[9] S. Yan, D. A. Huse and S. R. White, Science **332**, 1173 (2011); T. H. Han , J. S. Helton, S. Chu, D. G. Nocera, J. A. Rodriguez-Rivera, C. Broholm, and Y. S. Lee, Nature (London) **492**, 406 (2012); P. Mendels and F. Bert, J. Phys. Soc. Jpn. **79**, 011001 (2010).

[10] M. Hermele, M. P. A. Fisher, and L. Balents, Phys. Rev. B **69**, 064404 (2004).

[11] A. Banerjee, S. V. Isakov, K. Damle, and Y. B. Kim, Phys. Rev. Lett. **100**, 047208 (2008).

[12] N. Shannon, O. Sikora, F. Pollmann, K. Penc, and P. Fulde, Phys. Rev. Lett. **108**, 067204 (2012).

[13] L. Savary and L. Balents, Phys. Rev. Lett. **108**, 037202 (2012).

[14] O. Benton, O. Sikora, and N. Shannon, Phys. Rev. B **86**, 075154 (2012).

[15] For a recent review see C. Nisoli, R. Moessner, and P. Schiffer, Rev. Mod. Phys. **85**, 1473 (2013).

[16] C. L. Henley, Annu. Rev. Condens. Matter Phys. **1**, 179 (2010).

[17] B. Sutherland, Phys. Lett. A **26**, 532 (1968).

[18] R. Youngblood, J. D. Axe, and B. M. McCoy, Phys. Rev. B **21**, 5212 (1980).

[19] A. H. Castro Neto, P. Pujol, and E. Fradkin, Phys. Rev. B **74**, 024302 (2006).

[20] S. Chandrasekharan and U.-J. Wiese, Nucl. Phys. **B492**, 455 (1997); P. Orland and D. Rohrlich, Nucl. Phys. **B338**, 647 (1990).

[21] See Supplemental Material at http://link.aps.org/supplemental/10.1103/PhysRevLett.113.027204 (which includes Refs. [22–31]) for a detailed discussion of: (1) the mapping between the 16-vertex model and the Ising model on the checkerboard lattice; (2) the membrane algorithm; (3) the classical limit of quantum spin ice; (4) the thermal deconfinement transition in frustrated compact QED; (5) the degenerate perturbation theory for quantum square ice up to 8th order; (6) the probability distribution of the monopole or spinon separation; (7) the calculation of the dispersion of the spinon gap; (8) the visualization of the crossover from classical to quantum Coulomb phase; and (9) the gauge mean-field theory for quantum square ice.

[22] R. G. Melko and M. J. P. Gingras, J. Phys. Condens. Matter **16**, R1277 (2004).

[23] U. Wolff, Phys. Rev. Lett. **62**, 361 (1989).

[24] Y.-J. Kao and R. G. Melko, Phys. Rev. E **77**, 036708 (2008).

[25] L.-P. Henry and T. Roscilde (to be published).

[26] C. L. Henley, Phys. Rev. Lett. **62**, 2056 (1989).

[27] G.-W. Chern and R. Moessner, Phys. Rev. Lett. **110**, 077201 (2013).

[28] B. B. Beard, Nucl. Phys. B, Proc. Suppl.**73**, 748 (1999); V. Chudnovsky, Nucl. Phys. B, Proc. Suppl. **83–84**, 688 (2000).

[29] D. M. Ceperley, Rev. Mod. Phys. **67**, 279 (1995).

[30] C. Castelnovo, R. Moessner, and S. L. Sondhi, Phys. Rev. B **84**, 144435 (2011).

[31] M. Wallin, E. S. Sørensen, S. M. Girvin, and A. P. Young, Phys. Rev. B **49**, 12 115 (1994).

[32] A. M. Polyakov, *Gauge Fields and Strings* (Harwood Academic Publishers, Chur, Switzerland, 1987).

[33] N. Shannon, G. Misguich, and K. Penc, Phys. Rev. B **69**, 220403(R) (2004).

[34] O. F. Syljusen and S. Chakravarty, Phys. Rev. Lett. **96**, 147004 (2006).

[35] D. Banerjee, F.-J. Jiang, P. Widmer, and U.-J. Wiese, J. Stat. Mech. (2013) P12010.

[36] *Quantum Monte Carlo Methods in Condensed Matter Physics*, edited by M. Suzuki (World Scientific, Singapore, 1993).

[37] G. T. Barkema and M. E. J. Newman, Phys. Rev. E **57**, 1155 (1998).

[38] L.-P. Henry, P. C. W. Holdsworth, F. Mila, and T. Roscilde, Phys. Rev. B **85**, 134427 (2012).

[39] T. Kato, Prog. Theor. Phys. **4**, 514 (1949); D. J. Klein, J. Chem. Phys. **61**, 786 (1974).

[40] A term explicitly favoring the Néel states in the classical six-vertex model is the distinctive trait of the *F* model for antiferroelectricity [R. J. Baxter, *Exactly Solved Models in Statistical Mechanics* (Dover, New York, 2007)], and its competition with a plaquette-flip term in the quantum six-vertex model was considered previously in toy models, see, e.g., Refs. [33,34]. Here it is shown that the competition between these two terms dominates as well the low-energy physics of the microscopic model under consideration.

[41] Our constrained simulations can be regarded as a finite-temperature generalization of the approach recently introduced in Y. Tang and A. W. Sandvik, Phys. Rev. Lett. **110**, 217213 (2013) for the study of spinons induced in a variational wave function. See the Supplemental Material [21] for further details.

[42] V. N. Golovach, A. Minguzzi, and L. I. Glazman, Phys. Rev. A **80**, 043611 (2009).

[43] C. Schneider, D. Porras, and T. Schätz, Rep. Prog. Phys. **75**, 024401 (2012).

[44] A. A. Khajetoorians, J. Wiebe, B. Chilian, S. Lounis, S. Blügel, and R. Wiesendanger, Nat. Phys. **8**, 497 (2012).

[45] D. Banerjee, M. Dalmonte, M. Müller, E. Rico, P. Stebler, U.-J. Wiese, and P. Zoller, Phys. Rev. Lett. **109**, 175302 (2012).

[46] E. Zohar, J. I. Cirac, and B. Reznik, Phys. Rev. Lett. **109**, 125302 (2012).

[47] L. Tagliacozzo, A. Celi, A. Zamora, and M. Lewenstein, Ann. Phys. (Amsterdam) **330**, 160 (2013).